Application of micro–meso hierarchical porous carbon for toluene adsorption treatment

Fang Liu[1,*] ✉, *Xi Yan*[1,2,*], *Fengtao Fan*[1], *Chaocheng Zhao*[1], *Rentao Liu*[1], *Ya Gao*[1], *Yongqiang Wang*[1]

[1]*College of Chemical Engineering, China University of Petroleum, Qingdao 266580, People's Republic of China*
[2]*Department of environmental science and technology, SINOPEC Research Institute of Safety Engineering, Qingdao 266071, People's Republic of China*
[*]*These authors contributed to the work equally and should be regarded as co-first authors.*
✉ *E-mail: liufangfw@163.com*

Published in Micro & Nano Letters; Received on 22nd February 2016; Revised on 18th April 2016; Accepted on 19th April 2016

Organic waste gases from petrochemical industry cause air pollution. Due to the environmental effects of refractory organic gas, the development of effective adsorbent is imperative. The micro–meso hierarchical porous carbon with high surface area was synthesised by the hard-template method. With MCM-41 as template, this material was prepared using phenolic resin as carbon source. Dynamic adsorption performance of toluene on micro–meso hierarchical porous carbon was studied by gas chromatographic techniques. Effects of toluene initial concentration, temperature and bed height on adsorption capacity were also researched. The results showed that when toluene concentration was 1750 mg/m^3, equilibrium amount of toluene adsorbed was 358.8 mg/g by micro–meso hierarchical porous carbon, 79.41 mg/g by MCM-41. The adsorption capacity increased with the increase of initial concentration and bed height, while the adsorption capacity decreased along with the increase of temperature. Due to strong toluene adsorption capacity, this micro–meso hierarchical porous carbon manifests profound theoretical and practical significance in petrochemical organic waste gas treatment.

1. Introduction: Volatile organic compounds (VOCs) play an important role in air pollution, which cause harm to the environment or human health, even at low concentrations [1, 2]. One of the principal sources of VOCs is exhaust emission from petroleum industry. It includes benzene series, aldehydes and ketones compound, halohydrocarbon, alcohols and so on. The organic waste gases from petrochemical plants are mostly emitted by tanks inorganisation discharge, petrochemical unit leakage, solvent evaporation and exhaust emission [3]. Toxic, carcinogenic, diffusible and flammable, these organic compounds exert major concern even at low concentrations [4, 5]. Toluene, one representative kind of VOCs, is the most commonly found air pollutants emitted from petrochemical industries. Tiredness, confusion, nausea, memory loss, hearing and colour vision loss, appetite loss and neurological harm [6] can be caused when exposed to low concentration toluene. Hence, removal of toluene from emission streams is critical in air pollution control.

Significant scientific and technological efforts have been dedicated regarding organic compounds removal. The methods proposed and developed for treating VOCs are adsorption, absorption, catalytic oxidation, thermal oxidation, biological degradation method, condensation. Among them, the most extensively used is adsorption process [7–9]. It can provide better removal results at the low concentration of VOCs [10, 11]. Removal of organic compounds from emission gas can be carried out by various types of adsorbent.

Adsorbents can be divided by pore width into microporous adsorbents (<2 nm), mesoporous adsorbents (2–50 nm) and macroporous adsorbents (>50 nm) [12]. Adsorbents with high surface area and distinct pore structure must have high abrasion resistance and high thermal stability. Activated carbon (AC) is the most widely used adsorbent [13] due to its high surface area, microporous structure, a high degree of surface reactivity and hydrophobic properties [14, 15]. However, they are only useful for adsorbing molecules with molecular weights between 45 and 130 [1], since micropore adsorbents are not professionals when handling gaseous substances with macro molecules. The mesoporous molecular sieve MCM-41 possess various qualities such as large internal surface area, regular hexagonal array of uniform pore openings, narrow pore size distribution and tailorable pore size [16, 17]. However, MCM-41 may not be expected as an appropriate adsorbent for its amorphous mesoporous walls and poor thermal and hydrothermal stabilities [18]. Hence, appropriate adsorbents with high adsorption performance are necessary to be prepared for VOCs treatment.

In accordance with previous studies, sucrose as carbon precursor, ordered mesoporous carbons were synthesised using MCM-48 silica templates. However, carbon prepared using MCM-41 as a template collapses upon the template removal to yield high-surface-area disordered microporous structure. Current research focuses on the synthesis of ordered mesoporous carbon; application of carbon prepared by MCM-41 silica template has not been studied.

In this Letter, template synthesis technique is used to obtain micro–meso hierarchical porous carbon (MMHPC). The synthesis is performed using phenolic resin as carbon source and mesoporous molecular sieve MCM-41 as template. Carbon obtained has uniform mesopore distribution and disordered microporous structure. With high surface area, this carbon material combines the qualities of micro- and meso-porous molecular sieves. It can be used as adsorbent for both small and macro molecular substance emitted from petrochemical industry. The MMHPC has high abrasion resistance and high thermal stability. The toluene adsorption performances of the MMHPC have been evaluated.

2. Experiment

2.1. Materials: Mesoporous molecular sieve MCM-41 (Nankai University Catslyat Factory), and MMHPC (made in laboratory) were used in the experiment. Prior to use, these samples were subsequently dried at 110 °C for at least 24 h by vacuum drying oven to degas. Toluene (Sinopharm Chemical Reagent Corporation, analytical grade) was used as adsorbate.

2.2. Synthesis: The synthesis of MMHPC was performed using the mesoporous molecular sieve MCM-41 as the template. An aqueous solution of phenolic resin precursor with phenol/formaldehyde =

doi: 10.1049/mnl.2016.0058

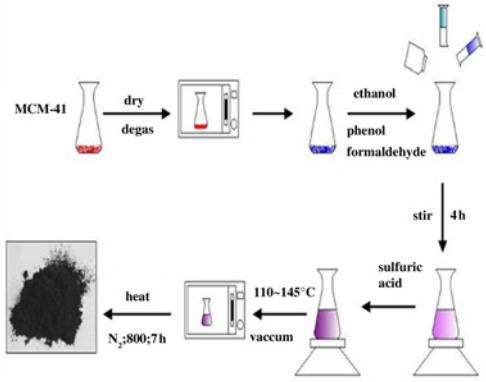

Fig. 1 *Synthesis process of MMHPC*

3.18 (15.0 mass% phenol, 4.7 mass% formaldehyde, 80.3 mass% ethanol) was used as the carbon source. The dehydrated silica molecular sieve was then impregnated with the aqueous solution. The suspension liquid was stirred continuously for 4 h in the temperature range of 40–80 °C. Using sulphuric acid as the catalyst, the suspension was then continuously stirred at 60 °C for 18–22 h. The mixed system was dried under vacuum for 24 h to a desired temperature in the range of 110–145 °C. After drying, the mixture was heated to 800 °C for 7 h under nitrogen atmosphere. Finally, the silica framework was removed by stirring in 2.5 wt% NaOH solution dissolved in 1:1 water–ethanol mixture by volume, at least twice at 373 K [19]. The synthesis process of MMPHC is presented in Fig. 1.

2.3. Characterisation: The morphologies of the samples were observed by a field-emission scanning electron microscope (SEM, Hitachi S-4800) equipped with energy dispersive spectrometer (EDS). The samples were observed by transmission electron microscopy (TEM, JEM-2100). Before the observation, powdered samples were dispersed in ethanol by ultrasonication for at least 5 min. Nitrogen sorption isotherms were measured with a Micromeritics ASAP 2020 at 77 K, and the samples were degassed at 523 K for at least 12 h in a vacuum line prior to the measurements. The surface areas were calculated through the Brunauer–Emmett–Teller (BET) method. The Barrett–Joyneer–Halenda method was utilised to measure mesopore size distributions. The micropore size distributions were analysed by the Horvath–Kawazoe method. The micropore surface area and micropore volume was estimated by *t*-plot method.

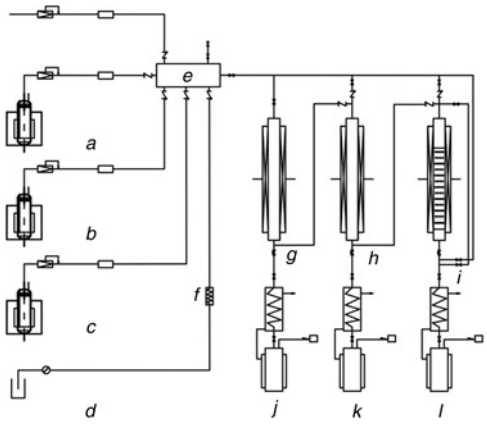

Fig. 2 *Toluene adsorption experimental device: (a–c) bubbling reactor, (d) air pump, (e) gas mixing apparatus, (f) gas flow controller, (g, h) fixed bed reactor, (i) fluidised bed reactor, (j–l) outlet*

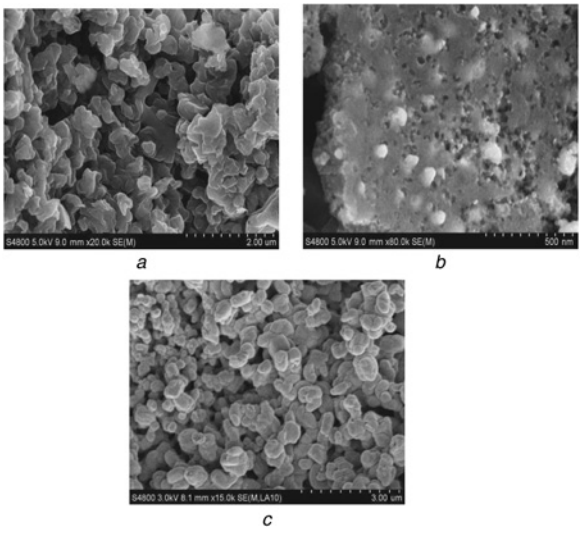

Fig. 3 *SEM images of adsorbents*
a MMHPC magnification ×20.0k
b MMHPC magnification ×80.0k
c MCM-41 magnification ×15.0k

2.4. Dynamic adsorption

2.4.1. Experimental device: The configuration of the adsorption system is shown in Fig. 2. The quartz glass cylindrical reactor (fixed bed reactor) of this system (g/h) is 250 mm in length and 20 mm in internal diameter. In a typical experiment, air is introduced to the system from an air pump (d), toluene vapour is generated from a bubbling reactor (a). The air flow rate (200 ml/min) and the concentrations of toluene vapour are controlled by the gas flow controller (f). The mixed gas sample and adsorption-treated gas sample can be collected by 100 ml glass injector from the dynamic gas mixing apparatus (e) and outlets (j/k), respectively.

2.4.2. Experimental methods: The adsorption behaviours of toluene on adsorbents (MMHPC and MCM-41) were studied. Before each adsorption experiment, samples were outgassed under vacuum at the temperature of 110 °C for at least 12 h. The effects of toluene concentration, temperature and bed height were researched. The concentrations of toluene were controlled in the range between 389 and 3869 mg/m^3. The temperatures used for the adsorption experiments were 25, 35 and 45 °C. Bed heights were in the range 5–15 mm. Gas chromatography (SP-3420A) was utilised to measure the toluene concentrations. The amount of toluene adsorbed on the adsorbents (q_e) was determined from the initial adsorption column weight and the saturated adsorption column weight (calculated by analytic balance) by the following equation

$$q_e = \frac{m_e - m_0}{m_0} \tag{1}$$

where m_0 (mg) and m_e (mg) are the mass of the initial and saturated adsorption column, respectively.

In the adsorption curve, the breakthrough time was defined when the output concentration (C) reached 10% of the inlet concentration (C_0) (min), and the saturation time was defined when the output concentration (C) reached 95% of the inlet concentration (C_0) (min).

3. Results and discussion

3.1. Material properties: The appearances of MCM-41 and MMHPC observed by a SEM are shown in Fig. 3. The club shaped morphology for the silica template MCM-41 with uniform particle size is shown in Fig. 3*c*. The SEM photographs show that MMHPC possess layered and porous structure.

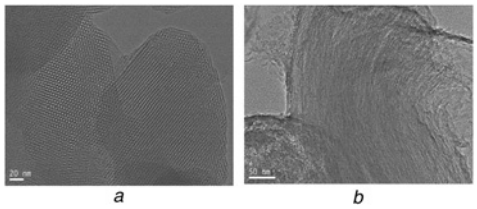

Fig. 4 *Transmission electron microscope images of adsorbents*
a MCM-41
b MMHPC

The TEM of MCM-41 gives the regular pore image in Fig. 4*a*. The TEM image shows that MCM-41 has a uniform pore distribution and regular hexagonal array of uniform channels [20, 21]. Fig. 4*b* shows uniform mesopore distribution of MMHPC. The elemental analysis of MMHPC is shown in Fig. 5 by energy dispersive spectromicroscopy (EDS). EDS indicates that MMHPC has partly ordered mesopore structure with silica framework removed.

Fig. 6 presents the nitrogen adsorption isotherms of MCM-41 and MMHPC. The uniform pronounced capillary condensation step of MCM-41 and MMHPC exhibits a type IV isotherm according to International Union of Pure and Applied Chemistry (IUPAC) classification [22]. The presence of hysteresis loop is corresponding to essentially mesoporous materials [23]. The pore structural parameters of the adsorbents obtained from the interpretation of nitrogen isotherm are given in Table 1. From Fig. 6 and Table 1, it can be observed that the adsorbents show different surface area, pore volume and microporous ratio. MCM-41 shows the large pore volume and the small micropore volume. MMHPC possesses the largest micropore volume.

Fig. 7 depicts pore size distributions for adsorbents. The adsorbents have different porosity distributions. MCM-41 possesses rich amount of mesopores at around 2.85 nm. MMHPC has both micropores (with peaks around 0.40–0.60 and 1.20–1.40 nm) and small mesopores at around 3.7 nm.

3.2. Adsorbing toluene properties of adsorbents: Adsorption experiments for toluene, 1750 mg/m^3 (C_0), with MCM-41 and MMHPC were carried out. The temperature used for the experiments was 25 °C. The fixed bed reactor was filled with 1 cm adsorbents. The adsorption capacities of MCM-41 and MMHPC under this condition are presented in Table 2 and the adsorption curves are shown in Fig. 8. Fig. 8 and Table 2 indicate that MCM-41 and MMHPC have different adsorption toluene capacities. Table 2 also summarises the amount of toluene adsorbed on the three adsorbents at equilibrium and the breakthrough time ($C/C_0 = 0.1$) and the saturation time ($C/C_0 = 0.95$). For MMHPC, the adsorption capacity for toluene is 358.8 mg/g, much higher than that of MCM-41 (79.41 mg/g). The

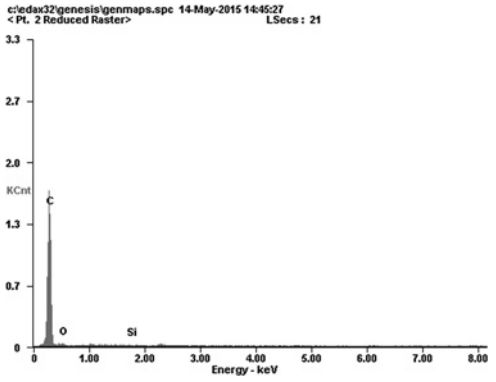

Fig. 5 *Energy dispersive spectromicroscopy of MMHPC*

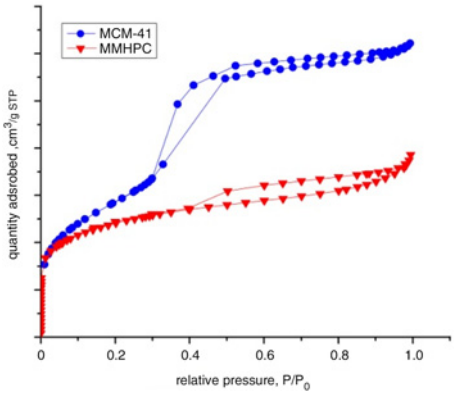

Fig. 6 *Nitrogen adsorption–desorption isotherms at 77 K for adsorbents*

breakthrough time for MCM-41 and MMHPC is 31 and 62 min, respectively. It can be found that MMHPC shows higher saturation adsorption capacity (358.8 mg/g) and longer saturation time (207 min) compared with MCM-41 (79.41 mg/g, 111 min).

From Table 1 it can be concluded that microporous volume and average pore size are the main parameters that control toluene adsorption capacity [24]. Also, the BET surface area is the key parameter for controlling toluene adsorption capacity in this research, which is consistent with Yang Jiao's research [25]. With large microporous volume, MMPHC has large toluene adsorption amount, which shows that micropores are beneficial to toluene adsorption. It can be concluded that the amount of toluene adsorbed is largely dependent on the micropore volume, because toluene molecule size is suitable for adsorption in micropores [26, 27]. Thus, it is concluded that adsorbents with large specific surface area, suitable micropore volume and proper pore size distribution are considered to have higher toluene adsorption capacity [28].

3.3 Effects of operation factors on toluene adsorption

3.3.1 Effect of inlet concentration on toluene adsorption: Adsorption curves were obtained by allowing diluted toluene gas at 200 ml/min at 25 °C to flow through a column where synthesised C1 were packed. Fig. 9 shows the effect of initial concentration (C_0) on toluene adsorption over 1 cm MMHPC. The temperature of these experiments is kept at 25 °C. It can be found that the curvilinear trend of the five adsorption curves is obviously identical. The output concentration is low at the beginning, because of the large surface area and abundant micropores. After the breakthrough point ($C/C_0 = 0.1$), a more rapid increase in these curves could be observed. This demonstrates that toluene adsorption capacity decreases with the amount of adsorbed toluene. It is shown in Table 3 that toluene amount increases with initial concentration changing from 389 to 3869 mg/m^3. The higher initial concentration leads to the shorter breakthrough time and saturation time. This may be due to the fact that when initial concentration increases, the mass transfer resistance become higher, which results in insufficient contact between the adsorbate (toluene) and the adsorbent (MMHPC) [29, 30].

Table 1 Pore structure characteristic of the adsorbents

Adsorbent	MCM-41	MMHPC
S_{BET}, m^2/g	1043.10	859.82
S_{mic}, m^2/g	0	751.64
S_{meco}, m^2/g	1043.10	108.18
V_{total}, ml/g	0.92	0.43
V_{mic}, ml/g	0	0.37
Average pore size/(nm)	2.86	3.96

doi: 10.1049/mnl.2016.0058

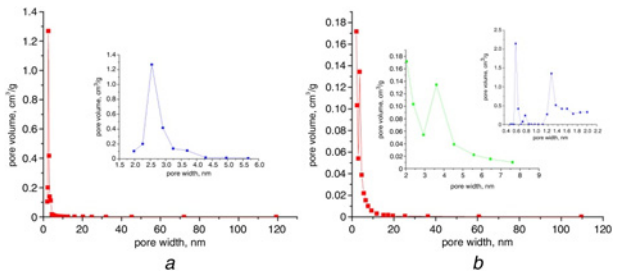

Fig. 7 *Pore size distributions of adsorbents*
a MCM-41
b MMHPC

3.3.2 Effect of temperature on toluene adsorption: Fig. 10 reflects the effect of temperature on toluene adsorption over MMPHC of 1 cm when the initial toluene concentration was 1750 mg/m^3. It is found that the higher the temperature is, the steeper the adsorption curve is, and the shorter the saturation time is. It can be seen from Table 4 that the saturated amount of toluene adsorbed decreases from 358.8 to 246 mg/g with experiment temperature increasing. The reason may be attributed to the intraparticle resistance of toluene molecules [31]. The motion of toluene molecules increases with temperature, which lead to stronger intraparticle resistance. Thus, toluene molecules are hard to be captured by the adsorbents.

3.3.3 Effect of bed height on toluene adsorption: Fig. 11 is obtained by allowing 1750 mg/m^3 of toluene at 200 ml/min to flow through a column where MMHPC was packed at 25 °C. From Fig. 11 and Table 5, it can be concluded that the higher the bed height is, the flatter the adsorption curve is, which results in longer breakthrough and saturation time. The amount of saturated toluene adsorption increases with the increase of bed height. This may be due to the fact that the higher the bed height is, the larger the amount of the adsorbents is, which leads to higher toluene adsorption capacity.

3.4 Toluene adsorption isotherm: The toluene adsorption isotherm on MMPHC is shown in Fig. 12. It can be concluded that the dynamic adsorption performance for gaseous toluene depends both on micropores and mesopores. The gaseous toluene is directly adsorbed into the micropores of MMPHC, leading to a sharp increase in the toluene adsorption isotherm at low concentrations (<2000 mg/m^3). Then the gaseous toluene passes through the inside of the mesopores, which causes a flatter increase (2000–3000 mg/m^3) in the toluene adsorption isotherm. Then another sharp increase (>3000 mg/m^3) in the toluene adsorption isotherm indicates that the gaseous toluene is rapidly adsorbed into the mesopores of MMHPC.

Adsorption isotherm is important in describing the interaction of solutes and adsorbent and how to optimise the use of the adsorbents. The Langmuir and Freundlich models were utilised to correlate the experimental data of toluene adsorption. Langmuir equation [32] is the most useful isotherm for both physical and chemical adsorption. It is represented as

$$\frac{1}{q_e} = \frac{1}{K_L q_m} \times \frac{1}{C_0} + \frac{1}{q_m} \tag{2}$$

Table 2 Toluene adsorption capacities of adsorbents at 1750 mg/m^3

Adsorbent	Toluene adsorbed amount, mg/g	Breakthrough time, min	Saturation time, min
MCM-41	79.41	31	111
MMHPC	358.8	62	207

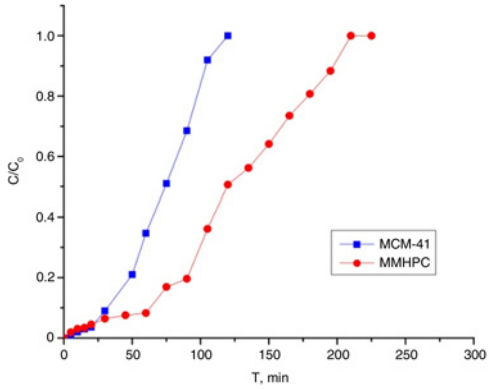

Fig. 8 *Breakthrough curves for toluene adsorption over 1 cm of the adsorbents*

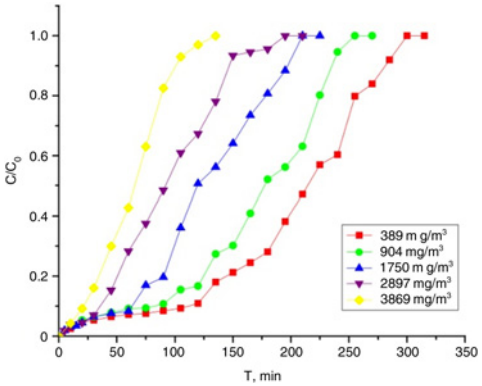

Fig. 9 *Effect of initial concentration on toluene adsorption*

Table 3 Toluene adsorption parameters onto MMHPC at different concentrations

Initial concentration, mg/m	Breakthrough time, min	Saturation time, min	Toluene adsorbed amount, mg/g
389	111	291	197
904	82	241	288.6
1750	62	207	358.8
2867	35	171	381.9
3869	21	113	426.5

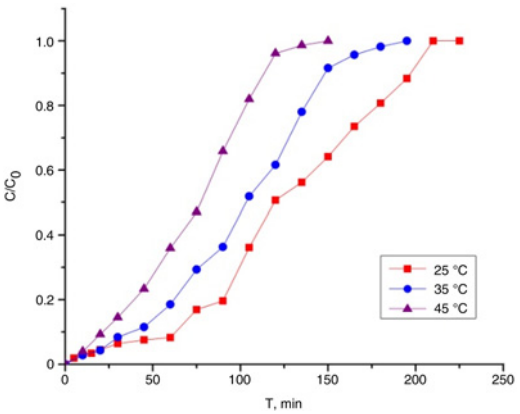

Fig. 10 *Effect of temperature on toluene adsorption*

Table 4 Toluene adsorption parameters onto MMPHC at different temperature

Temperature, °C	Breakthrough time, min	Saturation time, min	Toluene adsorbed amount, mg/g
25	62	207	358.8
35	38	163	287.3
45	21	119	246

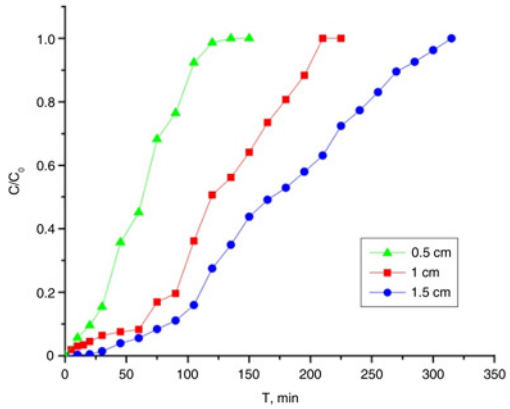

Fig. 11 *Effect of bed height on toluene adsorption*

Table 5 Toluene adsorption parameters onto MMPHC at different bed heights

Bed heights, mm	Breakthrough time, min	Saturation time, min	Toluene adsorbed amount, mg/g
5	21	111	218.5
10	62	207	358.8
15	84	295	432.9

where q_e and q_m are the maximum adsorption capacity (mg/g) and the adsorbed quantity (mg/g), respectively. K_L is the Langmuir constant. C_0 is the equilibrium concentration (mg/m^3).

Freundlich isotherm [33] is an empirical equation utilised to describe adsorption, usually written as

$$\lg q_e = \frac{1}{n}\lg C_0 + \lg K_F \tag{3}$$

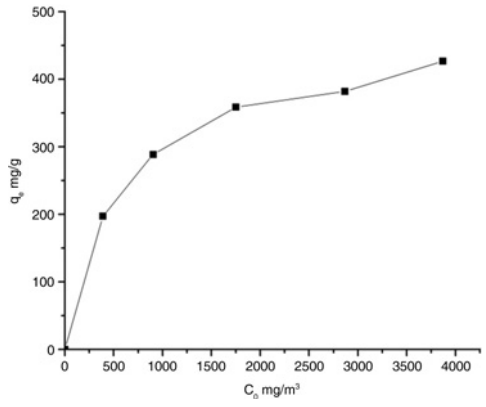

Fig. 12 *Toluene adsorption isotherm on MMHPC*

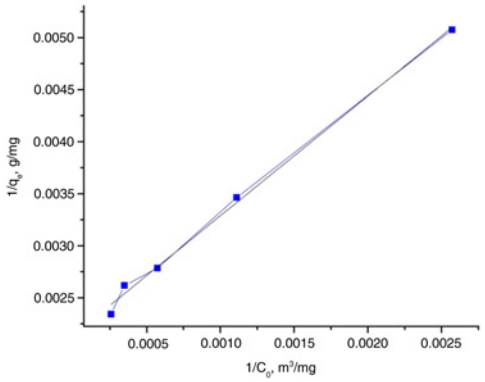

Fig. 13 *Langmuir isotherm fitting curve*

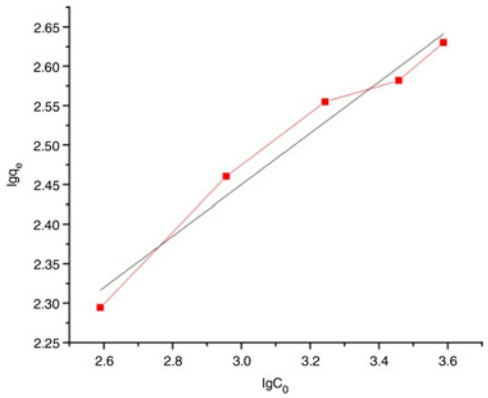

Fig. 14 *Freundlich equation fitting curve*

Table 6 Relative parameters of Langmuir equation and Freundlich equation

Langmuir			Freundlich		
q_m	K_L	R^2	n	K_F	R^2
467.29	0.001862	0.99519	3.07	29.81	0.95889

where K_F and n are empirical constants. C_0 is the equilibrium concentration (mg/m^3). The fitting curves are shown in Figs. 13 and 14, respectively.

From Figs. 13 and 14, it can be observed that adsorption isotherm of toluene on MMHPC fits Langmuir equation better. Table 6 presents that the correlation coefficient R^2 are 0.99519 and 0.95889 (lager than 0.95), respectively, which means that the adsorption isotherm of toluene can fit both Langmuir equation and Freundlich equation. For the R^2 of Langmuir equation is larger, adsorption isotherm of toluene on MMHPC fits Langmuir isotherm better. This may be because that the adsorption active sites distribute evenly on the surface of MMHPC.

4. Conclusion: To diminish the effects of refractory organic gas on the environment, the effective adsorbent has been developed by hard-template method. The main conclusions are shown as follows:

(i) The MMHPC has been synthesised using MCM-41 as hard template and phenolic resin as carbon source. The MMHPC has a surface area of 859.8204 m^2/g, a large micropore volume of 0.367725 ml/g and ordered mesopore stucture.

doi: 10.1049/mnl.2016.0058

(ii) The synthesised MMHPC shows better toluene adsorption performance than MCM-41 and commercial AC. When the toluene concentration is 1750 mg/m^3, an excellent toluene adsorption capacity of 358.8 mg/g at 25 °C is obtained.

(iii) Large surface area, large volume of narrow microporosity and proper average pore size are the desired parameters to achieve strong toluene adsorption capacities.

(iv) The amount of toluene adsorbed on the MMHPC increases with initial toluene concentration and bed height, and decreases with temperature. While the breakthrough time decreases with initial toluene concentration and temperature, and increases with bed height.

(v) The data obtained from the adsorption experiments are correlated with both Langmuir equation (0.99519) and Freundlich equation (0.95889). The adsorption isotherm of toluene on the MMHPC fits the Langmuir isotherm better.

5. Acknowledgment: This research was financially supported by the Top Talents Project of China University of Petroleum.

6. References

[1] Dolidovich A.F., Akhremkova G.S., Efremtsev V.S.: 'Novel technologies of VOC decontamination in fixed, moving and fluidized catalyst-adsorbent beds', *Can. J. Chem. Eng.*, 1999, **77**, (2), pp. 342–355

[2] Twumasi E., Forslund M., Norberg P., *ET AL.*: 'Carbon–silica composites prepared by the precipitation method, effect of the synthesis parameters on textural characteristics, and toluene dynamic, adsorption', *Porous Mater. J.*, 2012, **19**, (3), pp. 333–343

[3] Rao P.S., Ansari M.F., Gajrani C.P., *ET AL.*: 'Atmospheric concentrations of sulphur dioxide in and around a typical Indian petroleum refinery', *Bull. Environ. Contam. Toxicol.*, 2006, **77**, (2), pp. 274–281

[4] Martínez de Yuso A., Izquierdo M.T., Rubio B., *ET AL.*: 'Adsorption of toluene and toluene–water vapor mixture on almond shell based activated carbons', *Adsorption*, 2013, **19**, (6), pp. 1137–1148

[5] Baur G.B., Beswick O., Spring J., *ET AL.*: 'Activated carbon fibers for efficient VOC removal from diluted streams: the role of surface functionalities', *Adsorption*, 2015, **21**, (4), pp. 255–264

[6] Devathasan G., Low D., Teoh P.C., *ET AL.*: 'Complications of chronic glue (toluene) abuse in adolescents', *Aust. N.Z. J. Med.*, 1984, **14**, (1), pp. 39–43

[7] Adachi A., Ozaki H., Kasuga I., *ET AL.*: 'Use of beer bran as an adsorbent for the removal of organic compounds from wastewater', *Agric. Food Chem.*, 2006, **54**, (17), pp. 6209–6211

[8] Rytwo G., Gonen Y.: 'Very fast sorbent for organic dyes and pollutant', *Colloid Polym. Sci.*, 2006, **284**, pp. 817–820

[9] Lin C.-L., Cheng Y.-H., Liu Z.-S., *ET AL.*: 'Adsorption and oxidation of high concentration toluene with activated carbon fibers', *J. Porous Mater.*, 2013, **20**, (4), pp. 883–889

[10] Ruddy E.N., Carroll L.A.: 'Select the best VOC control strategy', *Chem. Eng. Prog.*, 1993, **89**, (7), pp. 28–35

[11] Foster K.L., Fuerman R.G., Economy J.: 'Adsorption characteristics of trace volatile organic compounds in gas streams onto activated carbon fibers', *Chem. Mater.*, 1992, **4**, (5), pp. 1068–1073

[12] Sing K.S.W., Everett D.H., Haul R.A.W.: 'Reporting physisorption data for gas/solid systems with special reference to the determination of surface area and porosity (Recommendations 1984)', *Pure Appl. Chem.*, 1985, **57**, p. 603

[13] Kim K.J., Kang C.S., You Y.J., *ET AL.*: 'Adsorption desorption characteristics of VOCs over impregnated activated carbons', *Catal. Today*, 2006, **111**, (3/4), pp. 223–228

[14] Bansal R.C., Goyal M.: 'Activated carbon adsorption' (CRC Press, 2005), p. 520

[15] Yu C., Qiu J.S., Sun Y.F., *ET AL.*: 'Adsorption removal of thiophene and dibenzothiophene from oils with activated carbon as adsorbent: effect of surface chemistry', *J. Porous Mater.*, 2008, **15**, (2), pp. 151–157

[16] Horcajada P., Ra'mila A., Pe'rez-Pariente J., *ET AL.*: 'Influence of pore size of MCM-41 matrices on drug delivery rate', *Microporous Mesoporous Mater.*, 2004, **68**, (1/2/3), pp. 105–109

[17] Marzouqa1 D.M., Zughul M.B., Taha M.O., *ET AL.*: 'Effect of particle morphology and pore size on the release kinetics of ephedrine from mesoporous MCM-41 materials', *J. Porous Mater.*, 2012, **19**, (5), pp. 825–833

[18] Mody H.M., Kannan S., Bajaj H.C., *ET AL.*: 'A simple room temperature synthesis of MCM-41 with enhanced thermal and hydrothermal stability', *J. Porous Mater.*, 2008, **15**, (5), pp. 571–579

[19] Ryoo R., Joo S.H., Kim J.M.J.: 'Energetically favored formation of MCM-48 from cationic–neutral surfactant mixtures', *Phys. Chem. B*, 1999, **103**, (35), pp. 7435–7440

[20] Beck J.S., Vartuli J.C., Roth W.J., *ET AL.*: 'A new family of mesoporous molecular sieves prepared with liquid crystal templates', *J. Am. Chem. Soc.*, 1992, **114**, pp. 10834–10843

[21] Szegedi Á., Popova M., Lázár K.: 'Influence of the acid/base and redox properties of catalysts in the gas-phase dehydration–dehydrogenation of cyclohexanol on iron and titania containing mesoporous materials', *J. Porous Mater.*, 2011, **104**, (2), pp. 291–301

[22] Gregg S.J., Sing K.S.W.: 'Adsorption, surface area and porosity' (Academic Press, London, 1986)

[23] Payer K.R., Hammond K.D., Tompsett G.A., *ET AL.*: 'The effects of mechanical and thermal perturbations on states within the hysteresis of sorption isotherms of mesoporous materials', *J. Porous Mater.*, 2009, **16**, (1), pp. 91–99

[24] Yu M., Gong H., Chen Z., *ET AL.*: 'Adsorption characteristics of activated carbon for siloxanes', *J. Environ. Chem. Eng.*, 2013, **1**, pp. 1182–1187

[25] Jiao Y., Chou T., Akcora P.: 'Design of ion-containing polymer-grafted nanoparticles for conductive membranes', *Macromolecules*, 2015, **48**, (14), p. 4910

[26] Kosuge K., Kubo S., Takemori K.N.: 'Effect of pore structure in mesoporous silicas on VOC dynamic adsorption/desorption performance', *Langmuir*, 2007, **23**, (6), pp. 3095–3102

[27] Hernández M.A., Corona L., González A.I.: 'Quantitative study of the adsorption of aromatic hydrocarbons (benzene, toluene, and p-xylene) on dealuminated clinoptilolites', *Ind. Eng. Chem. Res.*, 2005, **44**, (9), pp. 2908–2916

[28] Jiang T., Zhong W., Jafari T., *ET AL.*: 'Siloxane D4 adsorption by mesoporous aluminosilicates', *Chem. Eng. J.*, 2015, **289**, pp. 356–364

[29] Gaur V., Sharma A., Verma N.: 'Preparation and characterization of ACF for the adsorption of BTX and SO2', *Chem. Eng. Process., Process Intensification*, 2006, **45**, (1), pp. 1–13

[30] Mohana N., Kannana G.K., Upendraa S., *ET AL.*: 'Breakthrough of toluene vapours in granular activated carbon filled packed bed reactor', *J. Hazard. Mater.*, 2009, **168**, (2/3), pp. 777–781

[31] Huang Z.H., Kang F., Liang K.M., *ET AL.*: 'Breakthrough of methyethylketone and benzene vapors in activated carbon fiber beds', *J. Hazard. Mater.*, 2003, **98**, (17), pp. 107–115

[32] Langmuir I.: 'The adsorption of gases on plane surfaces of glass, mica and platinum', *J. Am. Chem. Soc.*, 1918, **40**, pp. 1361–1402

[33] Freundlich H.: 'Colloid and capillary chemistry, English translation of 3rd Germaned' (Methuen, London, 1926)